STRUCTURAL PARAMETER OPTIMIZATION AND TESTING OF LIQUID FERTILIZER DEEP-FERTILIZATION MECHANISM WITH DEFORMED GEARS

Feng JINLONG[1], Li QICHAO[2]*, Li HUA[3], Tian LIQUAN[4]

Deep-fertilization mechanism with deformed gears is a core part of liquid fertilization applicator. The performance of the mechanism is subject to the motion trajectories and perpendicularity to soil of the spray fertilizer needles. A man-machine dialogue analysis software was designed using Visual Basic 6.0 based on the present kinematic mathematical model. This software can simultaneously show the trajectories and entering and exiting postures of the spray fertilizer needles under parameter changes, and then output the results of the hole size and perpendicularity to soil. With the hole size and perpendicularity to soil as the optimization target and the man-machine dialogue analysis software as the basis, an optimal parameter combination that can meet the designing requirement of the mechanism was obtained using Taguchi experiment design method, and the structural design, test bed processing and simulation of field hole pricking mechanism were conducted subsequently. Results show that the deep-fertilization mechanism with deformed gears under optimized parameters can meet the designing requirement of the mechanism.

Keywords: deep-fertilization mechanism; liquid fertilizer; hole; deformed gears; Hole width; experimental design; optimization

1. Introduction

Deep-fertilization mechanism is a key part of deep-fertilization liquid fertilizer applicator, which is also the final executing mechanism of applying liquid fertilizer into soil during fertilization of corns, beans and other crops. The hole size after pricking is a key indicator of the performance of the mechanism, which has direct effect on the fertilization quality and efficiency of deep-fertilization applicator. With a high perpendicularity to soil for pricking, the spray fertilizer needles are supposed to carry less soil, resulting in small holes.

1 Lecturer , College of Mechanical and Electrical Engineering, Lingnan Normal University, Zhanjiang 524048, China
2 *Associate professor, College of Mechanical and Electrical Engineering, Lingnan Normal University, Zhanjiang 524048, China, *Email: 37002165@qq.com
3 Associate professor , College of Mechanical and Electrical Engineering, Lingnan Normal University, Zhanjiang 524048, China
4 Associate professor, Key Laboratory of Crop Harvesting Equipment Technology of Zhejiang Province, Jinhua Polytechnic, Jinhua 321017, China

Therefore, the deep-fertilization mechanism with high perpendicularity to soil and smaller holes has become a development trend for liquid fertilization deep-fertilization mechanism. Currently there are mainly three types of deep-fertilization mechanisms, namely crank rocker mechanism, planetary elliptic gear mechanism, and all planetary elliptic gear mechanism. Of them, crank rocker mechanism has difficulty in controlling the inertia of the mechanism, resulting in enlarged holes in the soil and more soil carried by the spray fertilizer needles [1-2]; for planetary elliptic gear mechanism, and all planetary elliptic gear mechanism, the perpendicularity to soil and holes have been largely improved due to dynamic and kinematic optimization, but the effect is still not satisfying [3-6]. Therefore, this paper proposed a deep-fertilization with deformed gears. By adjusting the deformed coefficients and eccentric ratio, the deformed gears can realize the vertical and horizontal varying of transmission ratio and enlarge the range of it. Compared with other hole pricking mechanisms, the proposed mechanism presented higher perpendicularity to soil and smaller hole sizes.

In this study, a kinematic mathematical model was established and a man-machine dialogue analysis software was designed to optimize the parameters of pricking mechanism with deformed gears for liquid fertilizer injection. But this trial-and-error approach has problem in guaranteeing the accuracy of optimization. In light of this, we applied Taguchi experimental design method based on man-machine dialogue analysis software to proceed parameter design and optimization, and obtained an optimal parameter combination that can meet the designing requirement of the mechanism. Then 3D design and processing was conducted on the optimized parameters, and verification test of the deep-fertilization mechanism was performed on test bed.

2. Deep-fertilization mechanism with deformed gears

2.1 Structural characteristics and working principle

Fig. 1 shows the proposed deep-fertilization mechanism with deformed gears, which consists of five congruent deformed gears, one planet carrier, one pair of rocker arms and spray fertilizer needles. Two pairs of deformed gears were located at the two ends of the major axis of the central deformed solar gear. The planet carrier 1 is coaxially arranged with the central deformed gear 4. The planetary deformed gear6 is consolidated with the rocker arm with screw to be one component. And the spray fertilizer needles 3 were fixed to one end of the rocker arm. When the mechanism is working, the central deformed solar gear stays fixed, the planet carrier rotates and drives two intermediate deformed gears to revolve around the central deformed solar gear 4, and meanwhile the planetary deformed gears at two sides would make cyclical movements. The compound motion of all the points (including spray fertilizer needle point D) on the rocker

arm spray fertilizer needles, the clockwise rotational movement of the planetary deformed gears and the swing with the planetary deformed gears have constituted the special trajectories of the spray fertilizer needles. By using optimal structural parameters, the compound motion of the gears can satisfy the pricking requirements of the spray fertilizer needles.

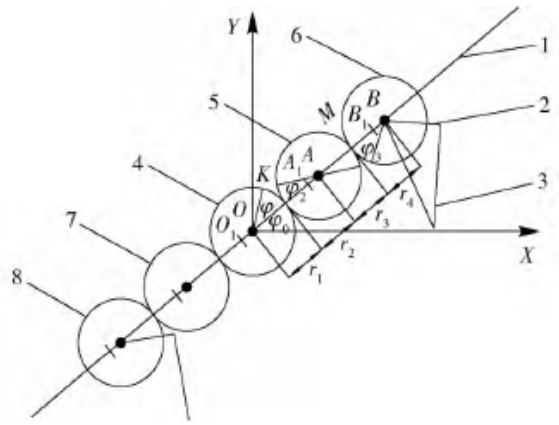

Fig. 1: Hole pricking mechanism with deformed gears
1. Planet carrier 2.Rocker arm 3.Spray fertilizer needle 4.Deformed solar gear 5.Upper intermediate deformed gear 6.Upper planetary deformed gear

2.2 Mathematical model of trajectories of spray fertilizer needles

Liquid fertilizer deep placement mechanism to rotate; the intermediate transformation gears 5 and 7 orbit the sun transformation gear 6 and rotate on their own axis, and the planetary transformation gears 4 and 8 are engaged with the intermediate transformation gears 5 and 7 respectively and orbit the sun transformation gear 6. As the planetary transformation gears are consolidated with the rocker arm and the fertilizer applicator, power will be ultimately transmitted to the fertilizer applicator to perform deep placement. When the planetary carrier of the mechanism rotates on its axis once, two fertilizer deep placements are performed. One revolution of the transformation gear liquid fertilizer deep placement mechanism and two deep placements can enormously improve the work efficiency. Since the transformation gears that make up the liquid fertilizer deep placement mechanism are arranged symmetrically around the center, the mechanism has less inertia. Hence, using transformation gears can realize good earth-entry trajectory, stable operation and compact structure.

The kinematics of the in-depth liquid fertilizer injection mechanism based on deformed gears is analyzed, and a XOY-coordinate system is established as shown in Figure 1. Because of the central symmetry of the planetary gear train, only one side is depicted. Define O as the rotation center of planet carrier, also

known as the sun deformed gear center, A as the rotation center of the intermediate deformed gear, B as the rotation center of the upper planet deformed gear, O, A, B as the focus points of the deformed gear and centers of rotation, respectively, and O_1, A_1, B_1 as other focus points of the corresponding deformed gear. The sun deformed gear is fixed to the carrier and remains stationary at work. The long axis OO_1 of the sun deformed gear is the initial position for the planet carrier to rotate. Define the initial included angle between OO_1 and the X -coordinate as φ_0, and the rotation angle of the planet carrier as φ. It is defined that the planet carrier rotates counterclockwise relative to the initial position as a positive value. K and M are the meshing points between the sun deformed gear and the upper and intermediate deformed gears. Then the pitch curve equations r_1 and r_2 of the deformed gear can be obtained by the following formula:

$$r_1=\begin{cases}\dfrac{a(1-e^2)}{1-e\cos(-m_1\varphi)} & (0\geq\varphi\geq-\dfrac{\pi}{m_1})\\ \dfrac{a(1-e^2)}{1-e\cos(\dfrac{m_1}{2m_1-1}(2\pi+\varphi))} & (-\dfrac{\pi}{m_1}>\varphi>2\pi)\end{cases} \tag{1}$$

$$r_2=2a-r_1 \tag{2}$$

In order to ensure that the two pitch curves of the deformed gear are closed, m_1 and m_2 should meet:

$$2\pi-\frac{\pi}{m_1}=\frac{\pi}{m_2} \tag{3}$$

The long axis AA_1 of the above intermediate deformed gear is the initial position of the planet carrier. Assuming that the upper intermediate deformed gear is fixed and the planet carrier rotates counterclockwise relative to the upper intermediate deformed gear at the rotation angle φ_2 (φ_2 >0), then φ_2 :

$$\varphi_2=\begin{cases}\dfrac{2}{m_1}\arctan(\dfrac{1+e}{1-e}\tan\dfrac{-m_1\varphi}{2}) & (0\geq\varphi\geq-\dfrac{\pi}{m_1})\\ 2\pi-\dfrac{4m_1-2}{m_1}\arctan(\dfrac{1+e}{1-e}\tan\dfrac{m_1(2\pi+\varphi)}{4m_1-2}) & (-\dfrac{\pi}{m_1}>\varphi>2\pi)\end{cases} \tag{4}$$

The long axis BB_1 of the above planetary deformed gear 6 is the initial position of the planet carrier. Assuming that the upper planetary deformed gear 6 is fixed, the planetary carrier rotates clockwise relative to the upper planetary deformed gear at the angle φ_3 (φ_3 <0). M is the meshing point between the upper intermediate deformed gear 5 and the upper planetary deformed gear 6. The pitch curve equations r_4 and r_3 of the deformed gear and φ_3 can be gained by the following formula:

$$r_4=\begin{cases}\dfrac{a(1-e^2)}{1-e\cos(m_1\varphi_3)} & (0\le\varphi_3\le\dfrac{\pi}{m_1})\\ \dfrac{a(1-e^2)}{1-e\cos(\dfrac{m_1}{2m_1-1}(2\pi-\varphi_3))} & (\dfrac{\pi}{m_1}\le\varphi_3\le 2\pi)\end{cases} \tag{5}$$

$$r_3=2a-r_4 \tag{6}$$

$$\varphi_3=\begin{cases}\dfrac{-2}{m_1}\arctan(\dfrac{1-e}{1+e}\tan\dfrac{m_1(\varphi_2+\pi)}{2}) & (0\le\varphi_2+\pi\le\dfrac{\pi}{m_1})\\ \dfrac{2}{m_1}(\dfrac{1-e}{1+e}\tan(\dfrac{m_1(2\pi-(\varphi_2+\pi))}{4m_1-2}) & (\dfrac{\pi}{m_1}\le\varphi_2+\pi\le 2\pi)\\ \dfrac{-2}{m_1}\arctan(\dfrac{1-e}{1+e}\tan\dfrac{m_1(\varphi_2-\pi)}{2}) & (0\le\varphi_2-\pi\le\dfrac{\pi}{m_1})\\ \dfrac{2}{m_1}(\dfrac{1-e}{1+e}\tan(\dfrac{m_1(2\pi-(\varphi_2-\pi))}{4m_1-2}) & (\dfrac{\pi}{m_1}\le\varphi_2-\pi\le 2\pi)\end{cases} \tag{7}$$

where r_3 is the distance from the rotation center of the intermediate deformed gear to M, the meshing point with the rotation center of the planetary deformed gear, mm; and r_4 is the distance from the rotation center of the planetary deformed gear to M, the meshing point with the intermediate deformed gear, mm.

The displacement of the rotation center B of the upper planetary deformed gear 6 is

$$\begin{cases}x_B=4a\cos(\varphi_0+\varphi)\\ y_B=4a\sin(\varphi_0+\varphi)\end{cases} \tag{8}$$

On the upper planetary deformed gear 6, the fertilizer spray needle 3 is fixedly assembled 2 with the rocker arm. The straight line BD formed by the upper planetary deformation gear rotation center B to the spray needle tip D takes the initial position of OB, and the initial angular displacement is α_0, then the angular displacement of BD is $\beta=\alpha_0+\varphi+\varphi_0-\varphi_3$.

The relative motion equation of the spray needle tip D is

$$\begin{cases}x_D=4a\cos(\varphi+\varphi_0)+h_2\cos\beta\\ y_D=4a\sin\cos(\varphi+\varphi_0)+h_2\sin\beta\end{cases} \tag{9}$$

where h_2 is Length of spray needle, mm.

When the mechanism moves at the speed of V_m, the absolute motion equation of the spray needle tip is

$$\begin{cases}x=x_D+V_m\varphi/\dot{\varphi}\\ y=y_D\end{cases} \tag{10}$$

Taking the derivative of Formula (8), we can have the velocity equation of the center of rotation B of the planetary transformation gears

$$\begin{cases} \dot{x}_B = -4a\dot{\varphi}\sin(\varphi_0+\varphi) \\ \dot{y}_B = 4a\dot{\varphi}\cos(\varphi_0+\varphi) \end{cases} \tag{11}$$

Taking the derivation of Formula (9), we have the velocity equation of the spray applicator tip D

$$\begin{cases} \dot{x}_D = -4a\dot{\varphi}\sin(\varphi_0+\varphi) - h_2(\dot{\varphi}-\dot{\varphi}_3)\sin\beta \\ \dot{y}_D = 4a\dot{\varphi}\cos(\varphi_0+\varphi) + h_2(\dot{\varphi}-\dot{\varphi}_3)\cos\beta \end{cases} \tag{12}$$

Taking the derivation of Formula (11), we have the acceleration equation of the center of rotation B of the upper planetary transformation gear:

$$\begin{cases} \ddot{x}_B = -4a\dot{\varphi}^2\cos(\varphi_0+\varphi) \\ \ddot{y}_B = -4a\dot{\varphi}^2\sin(\varphi_0+\varphi) \end{cases} \tag{13}$$

Taking the derivation of Formula (2), we have the angular acceleration equation of the upper middle transformation gear:

$$\ddot{\varphi}_2 = -\frac{2a\dot{\varphi}\dot{r}_1}{(2a-r_1)^2} \tag{14}$$

Taking the derivation of Formula (12), we have the acceleration equation of the spraying applicator tip D:

$$\begin{cases} \ddot{x}_D = -4a\dot{\varphi}^2\cos(\varphi_0+\varphi) - h_2(\dot{\varphi}-\dot{\varphi}_3)\cos\beta \\ \ddot{y}_D = -4a\dot{\varphi}^2\sin(\varphi_0+\varphi) - h_2(\dot{\varphi}-\dot{\varphi}_3)\sin\beta \end{cases} \tag{15}$$

3 Taguchi test design and optimization

3.1 Man-machine dialogue simulation software

Based on the established kinematic model, a kinematic simulation and optimization software of deep-fertilization mechanism with deformed gears was designed using Visual Basic6.0, as shown in Fig. 2. The input parameters of the software include the semi-major axis a of the deformed gears, the eccentric ratio e, the deformation coefficient m_1, the length of spray fertilizer needle h_2, the initial angle between the spray fertilizer and the major axis of the planetary deformed gear α_0, and so on [7-12]. According to agronomic requirements, for input parameters, the hole distance is set as $H=220mm$, and the initial angle of the planet carrier rotation is set as $\varphi_0=50^o$ according to the common installation angle of planet carrier; and the output parameters include hole size k and perpendicularity to soil θ_1. Each time when a set of parameters were input, the simulation software can calculate rapidly and update the absolute motion and relative motion trajectories of the hole pricking mechanism, and meanwhile output the hole size and perpendicularity to soil.

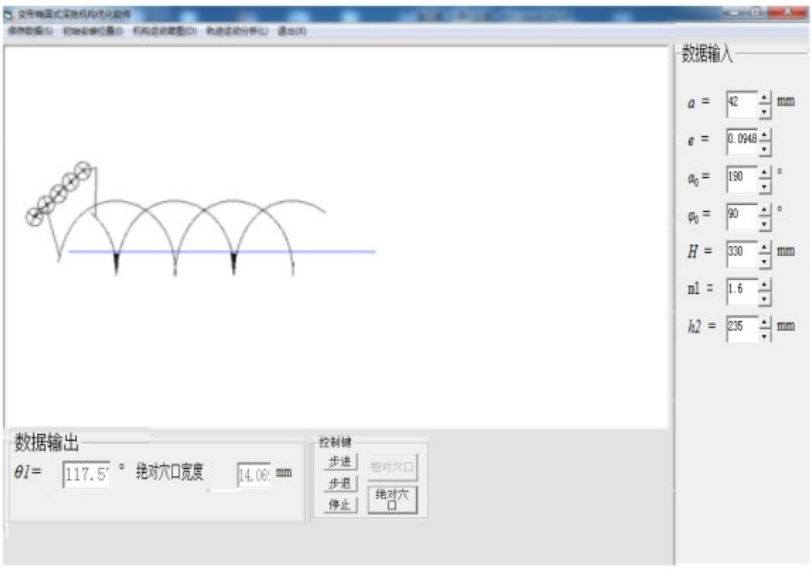

Fig.2: Optimization interface of visible man-machine interaction

3.2 Software-based Taguchi test design and optimization

Five parameters, namely the semi-major axis a, the eccentric ratio e, the deformation coefficient m_1, the length of spray fertilizer needle h_2 and the initial angle between the spray fertilizer needle and the major axis of the planetary deformed gear α_0, were selected as the factors of Taguchi test to investigate their impact on the output parameters of hole size k and perpendicularity to the soil θ_1. Based on design experience, four levels of the factors were selected for the test. The five-factor, four-level table of Taguchi test was shown as Tab. 1[13].

Table 1

Factor level table

Level	a/mm	e	α_0/(°)	m_1	h_2/mm
1	28	0.0618	105	1.2	140
2	29	0.0668	115	1.3	150
3	30	0.0718	125	1.4	160
4	31	0.0768	135	1.5	170

The test results based on Taguchitest scheme for L_{16} (4^5) and man-machine dialogue software were shown as Tab. 2.

Table 2

Test scheme and results for L16 (45)

Number	a/mm	e	α_0(°)	m_1	h_2/mm	k/mm	θ_1/(°)
1	4	3	2	4	1	34.59	117.8
2	1	3	3	3	3	37.27	108.8
3	1	1	1	1	1	35.55	130.5
4	4	1	4	2	3	31.93	99.3
5	4	2	3	1	4	28.18	110.9
6	1	4	4	4	4	59.70	98.0
7	3	3	1	2	4	32.74	129.9
8	2	2	1	4	3	31.63	127.6
9	2	1	2	3	4	28.10	118.3
10	2	3	4	1	2	28.95	101.3
11	3	1	3	4	2	28.67	107.4
12	2	4	3	2	1	20.62	109.9
13	4	4	1	3	2	37.21	129.1
14	3	4	2	1	3	28.35	121.7
15	1	2	2	2	2	29.44	119.6
16	3	2	4	3	1	31.02	98.5

The test results shown in Table 2 were analyzed using Design-Expert8.0.6 software [14]. The variance analysis results of the impact of each factor on the hole size k and perpendicularity to the soil$\theta_1$were shown as Table 3 and Table 4.

Table 3

Variance analysis of the impact of factors on hole size k

Impact factor	Quadratic sum	Degree of freedom	F value	Significance (P>F)
a	343.30	3	2.26	0.1342
e	129.94	3	1.49	0.2811
α_0	179.95	3	1.59	0.2879
m_1	202.33	3	1.35	0.4063
h_2	96.49	3	0	1.0000

Table 4

The factorial analysis of variance for earth-entry angle $\theta 1$/(°)

Impact factor	Quadratic sum	Degree of freedom	F value	Significance (P>F)
a	0.047	3	1.63	0.3497
e	1.48	3	23.80	0.0010
α_0	2004.53	3	32295.24	<0.0001
m_1	25.25	3	406.83	<0.0001
h_2	0.077	3	0	1.0000

The result was significant when P>F was less than 0.2. As shown in Tab. 3 and Tab. 4, the length of spray fertilizer needle h_2 has no impact on the hole size and perpendicularity to the soil; Tab. 3 shows that parameters a, e, $m_1$and $\alpha_0$have impact on the hole size; Tab. 4 shows that a, e, m_1 and α_0 have impact on the perpendicularity to the soil, and the impacts of $m_1$and $\alpha_0$were significant.

According to agronomic requirements, the hole size and the perpendicularity were taken as the indicator and the optimal target was constrained to realize better hole pricking efficiency, with perpendicularity being 90°-120° mm and hole size being 19-35mm. Design-Expert8.0.6 was applied for optimal solution. The optimal combination scheme with factors satisfying performance indicators based on designing requirements was shown as Tab. 5.

Table 5

Design-Expert optimal parameter combination

a mm	e	α_0 (°)	m_1	h_2 mm	Hole size k mm	Perpendicularity to the soil θ_1 (°)
30	0.0718	125	1.3	160	19.9	98.55

After inputting the optimized parameter combination separately into the man-machine interaction software, we can get the hole pricking trajectory and entering posture of the mechanism as shown in Fig. 3. The results indicate that the parameters of the deep-fertilization mechanism can satisfy the constraints.

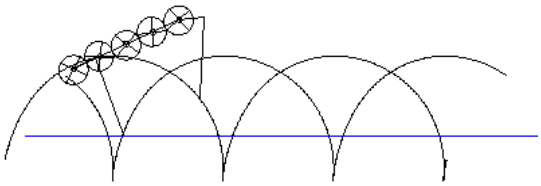

Fig. 3: Absolute hole pricking trajectory and entering posture simulation of deep-fertilization mechanism

4. Test

4.1 Virtual prototype test

Based on the parameter optimization of the mechanism, a structural design of the deep-fertilization mechanism with deformed gears was then conducted. A 3D solid model of the deep-fertilization mechanism with deformed gears was built using Pro/E software. Make the virtual assembly and introduce into ADAMS software for virtual prototype test [15-16]. The static trajectory of spray fertilizer needle point obtained from the virtual prototype test and theoretical analysis is shown as Fig. 4. The results show that the curve of the simulation is basically identical with that of the theoretical analysis, indicating that the design of the deep-fertilization mechanism is reasonable which can meet the anticipated goal.

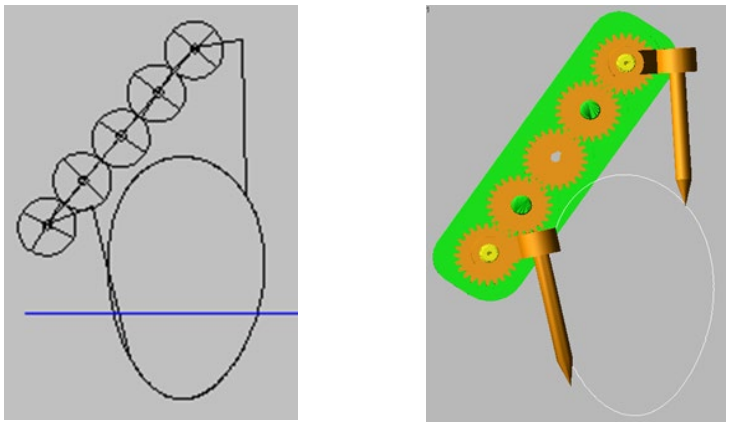

(a) Theoretical trajectory (b) Static trajectory of Adams simulation

Fig. 4: Comparison of theoretical trajectory and Adams simulation results

4.2 Simulation of field hole pricking test

To further verify the performance of the optimized injection-type liquid fertilizer deep-fertilization mechanism with deformed gears, a deep-fertilization mechanism test bed was designed to simulate the field hole pricking test, as shown in Fig. 5. The actually measured hole sizes were compared with the optimized results by the deep-fertilization mechanism. The testing site was in the farm tool laboratory of School of Engineering, Northeast Agricultural University.

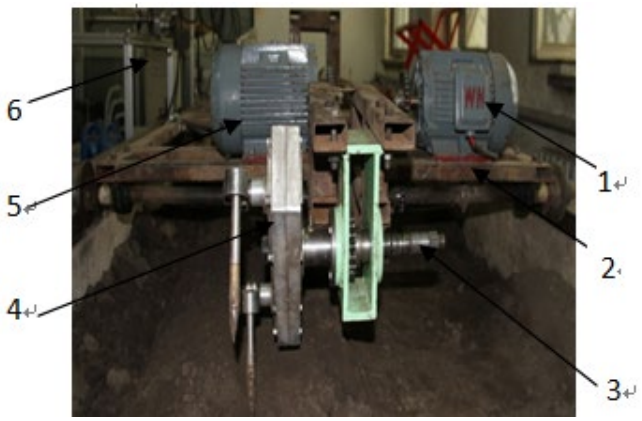

Fig. 5: Test bed of hole pricking mechanism

1. Motor (1) 2. Test bed rack 3. Gearing 4. Hole pricking mechanism with deformed gears 5. Motor (2) 6.Frequency conversion cabinet

On the test bed, the frequency conversion cabinet controls motor (1) and motor (2). Motor (1) controls the reciprocating motion of the test trolley on the soil-bin rail, and motor (2) controls the rotation of the hole pricking mechanism

with deformed gears through the gearing. Each rotation contains two hole pricking. During the test, the planet carrier speed was set as 80*r/min*. Totally five repeated tests were conducted, each test measuring ten holes. Take the average and the hole width results were shown as Tab. 6.

According to Tab. 6, the average hole width of the five repeated tests was 21.1mm, a 1.2 mm difference from the output parameter of 19.9 mm obtained by the simulated optimization analysis software of deep-fertilization mechanism with deformed gears. The difference between the soil environment and the ideal state is the major cause to the error of the test results. The actual hole size measurements were within the range of the agricultural requirement and can satisfy the hole pricking requirements of liquid fertilizer deep-fertilization applicator.

Table 6

Measurements of hole width

Test number	Width of hole (mm)										Average (mm)
	1	2	3	4	5	6	7	8	9	10	
1	21	20	22	22	20	20	20	21	21	22	20.9
2	23	21	21	22	20	20	22	21	21	21	21.2
3	22	22	20	20	21	20	21	21	21	20	20.8
4	21	21	20	21	21	22	22	20	21	21	21.0
5	21	21	22	21	22	22	21	22	22	20	21.4

5. Conclusion

(1) An injection-type liquid fertilizer deep-fertilization mechanism with deformed gears was proposed. This mechanism has high perpendicularity to soil and small hole size which can meet agricultural requirements. The composition and working principle of the deep-fertilization mechanism were analyzed and kinematic model of the mechanism was built.

(2) A simulation analysis software of the proposed deep-fertilization mechanism with deformed gears was designed using *Visual Basic* software. Based on man-machine dialogue analysis software, Taguchi test design method was applied to obtain the optimal parameter combination that can satisfy agricultural requirements. The parameters of the combination were: $a=30mm$, $e=0.0718$, $m_1=1.3$, $\alpha_0=125^o$ and $h_2=160mm$.

(3) Virtual simulation tests and simulated field hole pricking tests were conducted based on the optimized parameters. Results show that the average hole size was 21.1mm, which can meet the agricultural requirement.

Acknowledgments

Thank you for Postdoctoral Science Foundation of Heilongjiang Province of China (Grant No. LBH-Z18254), Guangdong basic and applied basic research

fund project (2021A1515011790), Special project for doctoral talents of Lingnan Normal University (ZL2021019).

REFERENCES

[1] *Wang, J.W., Zhou, W.Q., Bai, H.C., Wang, J.F., Huang, H.N., Wang, Z.B.,* Design and Experiment of Differential-type Bidirectional Distribution Device for Fertilizer Supply for Deep-fertilizer Liquid Fertilizer Application. Transactions of the Chinese Society for Agricultural Machinery, 49(6): 105-111, 2018.

[2] *Dixit, J., Kumar, V., Ali, M.,* Development and Evaluation of a Single Row Manual Vegetable Transplanter. Agricultural Engineering Today, 42(2): 58-66, 2018.

[3] *Zhou, C.J., Hu, B., Chen, S.Y., Ma, L.,* Design and analysis of high-speed cam mechanism using Fourier series. Mechanism and Machine Theory, 104: 118-129, 2016. https://doi.org/10.1016/j.mechmachtheory.2016.05.009

[4] *Zhang, L.B., Cai, Z.X., Wang, L.W., Zhang, R.X., Liu, H.F.,* Coupled Eulerian-Lagrangian finite element method for simulating soil-tool interaction. Biosystems Engineering, 175: 96-105, 2018. https://doi.org/10.1016/j.biosystemseng.2018.09.003

[5] *Wang, J.W., Zhou, W.Q., Wang, X.; Li, X., Wang, J.L., Li, S.W.,* Oblique type pricking hole mechanism based on lagrange curve for cubic fitting trajectory. Transactions of the Chinese Society for Agricultural Machinery, 48(5), 79–85, 2017.

[6] *Wang, J.F., Wang, J.W., Ju, J.Y., He, J.N.,* Research progress on pricking hole mechanism of deep-fertilization liquid fertilizer applicator. Journal of Northeast Agricultural University, 44(5): 157-160, 2013. DOI: 10.19720/j.cnki.issn.1005-9369.2013.05.030

[7] *Zhao, Y., Yu, G.H., Wu, C.Y.,* Numerical analysis and synthesis of mechanism [M]. Beijing: China Machine Press. 2005.

[8] *Li B.F.,* Agricultural machinery [M]. Beijing: China Agriculture Press. 2003.

[9] *Chen, J.N., Huang, Q.Z., Wang, Y., Zhang, G.F.,* Kinematics modeling and analysis of transplanting mechanism with planetary elliptic gears for pot seedling transplanter. Transactions of the Chinese Society of Agricultural Engineering, 28(5): 6-12, 2012.

[10] *Thomas, E.V.,* Development of a mechanism for transplanting rice seedlings. Mechanism and Machine Theory, 37(4):395-410, 2002.

[11] *Yu, G.H., Qian, M.B., Zhao, Y., Wu, C.Y.,* Analysis of Kinematic Principle of Transplanting Mechanism with Eccentric Gears and Non-circular Gears. Transactions of the Chinese Society for Agricultural Machinery, 40(3):81-84, 2009.

[12] *Yu, G.H., Chen, J.N., Zhao, F.Q., Zhao, Y.,* Dynamics Analysis of Transplanting Mechanism with Planetary Spur Gears. Transaction of the Chinese Society for Agricultural Machinery, 36(4), 51–55, 2015.

[13] *Wang, W.Z.,* Experimental design and analysis [M]. Beijing: Higher Education Press. 2004.

[14] *Xu, X.H., He, M.Z.,* Experimental design and application of Design-Expert and SPSS [M]. Beijing: Science Press. 2010.

[15] *Fan, C., Xiong, G.M., Zhou, M.F.,* Application and advancement of ADAMS [M]. Beijing: China Machine Press. 2006.

[16] *Chen, L.P., Zhang, Y.Q., Ren, W.Q.,* Mechanical system dynamics analysis and ADAMS application tutorial [M]. Beijing: Tsinghua University Press. 2005.